Tangential-force model for interactions between bonded colloidal particles

Volker Becker[*] and Heiko Briesen[†]

Max Planck Institute for Dynamics of Complex Technical Systems, Sandtorstrasse 1, D-39108 Magdeburg, Germany
(Received 22 August 2008; revised manuscript received 14 October 2008; published 22 December 2008)

Recently, Pantina and Furst [Phys. Rev. Lett. **94**, 138301 (2005)] experimentally demonstrated the existence of tangential forces between bonded colloidal particles and the capability of these bonds to supporting bending moments. We introduce a model to be used in computer simulations that describes these tangential interactions. We show how the model parameters can be determined from experimental data. Simulations using the model are in agreement to the measurement by Pantina and Furst. Application of the model to an aggregate with fractal structure leads to more realistic behavior than using classical approaches only.

I. INTRODUCTION

The structure of colloidal aggregates is important in various applications (e.g., pharmaceuticals, food processing, nanoparticle synthesis). To address structural aspects microsimulation of aggregating colloidal particles are an important and growing field in colloid science. Microsimulation of aggregates allows to investigate the structural evolution of aggregates by tracking the trajectories of the constituent primary particles. These trajectories are obtained from solving Newton's equation of motion for all the aggregates primary particles. In the future, insight in structure formation may be exploited to tailor aggregate structures by optimal process design. In the literature some work can be found on simulating aggregate structure evolution in hydrodynamic environments. Generally, one must distinguish the hydrodynamic and the particle interaction forces. Initial attempts of structural modeling have been carried out by Doi and Chen [1,2]. For the hydrodynamic forces they used the so-called free draining approximation according to which the hydrodynamics forces on the particles are strongly simplified. Each particle experiences only Stoke's drag force. Thus, all flow field perturbations induced by the particles, which potentially affect the flow around neighboring particles, are neglected. For the particle interaction they also used a simple model where sticking particles can roll on each other and the bond between two particles breaks if the normal forces exceed a critical value. Higashitani *et al.* [3] performed simulations, where the hydrodynamic and interparticle forces are considered in much more detail. Interparticle forces were obtained by the classical Derjaguin, Landau, Verwey, Oberbeek (DLVO) theory [4]. For particles in contact they used the model of Cundall and Strack [5] which is widely used in discrete element modeling of granular matter [6].

Regarding the hydrodynamic forces they accounted for screening of inner particles from the flow field by means of detailed geometrical computations. Similar studies have been done by Fanelli *et al.* [7,8] who also used a discrete element method (DEM) and DLVO forces to simulate dispersions of colloidal aggregates. Harada *et al.* [9] examined the structural change of nonfractal clusters. To compute the hydrodynamic forces they used Stokesian dynamics [10,11] which allow computation of the full, hydrodynamic interaction on the basis of the Stokes equation. As direct particle interactions they considered a retarded attractive van der Waals potential. Most of these studies assume normal forces between particles.

There are only a few simulation studies where non-normal forces are included. In the work by Higashitani *et al.* [3] the contact model of Cundall and Strack [5] is employed. That model is designed to capture sticking and sliding friction. However, as it will be shown, the classical Cundall-Strack model is not capable of qualitatively describing the experimentally observed behavior of bonded colloidal particles. In the field of disordered networks, e.g., gels and glassy structures, some models for tangential forces capable of supporting bending moments were derived (see, e.g.,[12–15]). Potanin [16] adopted the main ideas of these models to apply them in the context of colloidal aggregates. He used a Hamiltonian used in Born's model for the elasticity of microscopic networks [17]. This model was applied to the simulation of aggregates under static conditions but is not suited to describe the dynamic behavior, e.g., the rotation of an aggregate, correctly. In subsequent work [18], the author calculated the tangential forces based on a Hamiltonian derived by Kantor and Webman [14]. This Hamiltonian based on a three-body approach. The bending energy is proportional to the variation of the angle between two neighboring bonds. With this approach the breakage behavior of aggregates formed by diffusion limited cluster aggregation (DLCA) was investigated. However, this approach does not allow irreversible rearrangement of particles. Thus, the approach is restricted to situations where restructuring effects are irrelevant. West, Melrose, and Bell [19] presented another approach to include tangential and bending forces. They replaced the particles by a stiff trimer of particles and the basic colloidal bond was taken as a superimposition of 3×3 sphere interactions. Botet and Cabane [20] introduced a model where the bond between two spherical colloidal particles is described by springs which connect pins on the spheres surface. These pins are randomly distributed over the spheres. Whenever the distance between two pins on different spheres is smaller than a characteristic threshold, a spring between these pins will be initiated. The two pins cannot form another bond as long as the bond is present. If a spring

*becker@mpi-magdeburg.mpg.de
†briesen@mpi-magdeburg.mpg.de

exceeds a maximum elongation the spring will be destroyed. That spring causes both normal and tangential interaction between the spheres. A comparison of that model to the one proposed in this work will be given in Sec. IV C.

Recently, experimental evidence of bending moments has been presented by Pantina and Furst [21]. They measured that even a single bond is capable of supporting a bending moment. Except the model of Botet and Cabane [20], none of the above-mentioned models can describe both observed effects. In this paper we present a model to be used in DEM simulations which is able to describe the phenomena found by Pantina and Furst [21]. We furthermore show that all necessary model parameters can directly be obtained from their experiments. We will show that in some special cases our model reproduces the Hamiltonian used in [14] and we will compare our model to the models mentioned above.

The organization of the paper is as follows. Section II summarizes the basic experimental findings of Pantina and Furst regarding tangential forces as they are of major importance to the model developed in this contribution. In sec. III we will briefly revisit the classical DLVO forces. Section IV introduces the model for tangential forces, presents the method to determine the model parameters and compares our model to previous ones. Section V explains the basic simulation technique and shows simulation results. Finally, Sec. VI summarizes our findings and draws some conclusions.

II. EXPERIMENTAL OBSERVATIONS BY PANTINA AND FURST

In their experiments Pantina and Furst [21] used a linear chain of polymethylmethacrylate (PMMA) particles immersed in an $MgCl_2$ aqueous solution. The terminal particles of the chain were fixed by optical tweezers and the middle particle was pulled by another optical tweezers perpendicular to the chain direction. If only central forces acted between the particles the formation of a triangular structure can be expected. However, it turned out that the positions of the particles are in good agreement with the shape expected from a thin elastic rod

$$\frac{y(x)}{F_{\text{Bend}}} = -\frac{1}{EI}\left(\frac{L}{4}x^2 - \frac{|x|^3}{6}\right). \quad (1)$$

Here $y(x)$ is the deflection as a function of the position x, L is the length of the aggregate, E is the Young modulus, and I is the second moment of area. This is clear evidence that bonds between colloidal particles are capable of supporting bending moments. Furthermore, they measured the bending rigidity, κ, defined as the constant of proportionality between the deflection δ of the aggregate and the applied force,

$$F_{\text{Bend}} = \kappa\delta. \quad (2)$$

Additionally, they found that $\kappa \propto L^{-3}$ as expected from Eq. (1). The bending rigidity can be expressed by the relation

$$\kappa = \kappa_0\left(\frac{a}{L}\right)^3, \quad (3)$$

where a is the particle radius and κ_0 is the bending rigidity per bond. They measured these quantities as functions of the

$MgCl_2$ concentration. Furthermore they found that there is a critical bending moment M_c, above which the particle begins to slide and rearrangements of particles occurs.

Pantina and Furst [21] presented a possible explanation for the tangential forces in terms of the Johnson-Kendall-Roberts (JKR) theory for adhesive surfaces. They related the single bond rigidity κ_0 to the work of adhesion W_{sl} derived from the JKR theory and to the Young modulus of the particles. In subsequent work, Pantina and Furst [22] generalized that theory to the case that divalent ions are present. In that case ion bridges between the spheres appear which increases the attraction between the particles and leads to a higher bending rigidity.

III. DLVO FORCES

Let us briefly revisit the DLVO theory. The first ingredients of the DLVO theory are van der Waals forces. In the framework of the nonretarded Hamaker approximation, the mutual interaction potential between two particles can be found in standard literature (e.g.,[4,23]):

$$V(R)_{\text{vdw}} = -\frac{A}{6}\left[\frac{2a^2}{R^2-4a^2} + \frac{2a^2}{R^2} + \ln\left(\frac{R^2-4a^2}{R^2}\right)\right], \quad (4)$$

where R is the center-center distance between two particles and A is the Hamaker constant, depending on particles' and fluid's properties. The second ingredient is the electrostatic double layer theory. Here we use the Derjaguin approximation with the assumption of constant surface potential. The mutual interaction potential can again be found in the literature [4,23]:

$$V(R) = 2\pi\epsilon a\phi_0^2 \ln\{\exp[-\lambda(R+a)]\}. \quad (5)$$

Here ϵ is the electric permittivity of the carrier fluid, ϕ_0 is the surface potential, and λ is the Debye-Hueckel parameter defined as

$$\lambda = \sqrt{\frac{e^2}{\epsilon k_B T}\sum_{i=1}^{N} n_i z_i^2}, \quad (6)$$

where e is the elementary charge, k_B is the Boltzmann constant, T is the temperature, n_i is the ion concentration of the ith ion species, and z_i is the corresponding valency. The inverse of the Debye-Hueckel parameter is a measure for the magnitude of the screening length for electric fields in an electrolyte solution. Besides these standard ingredients we use an additionally repulsive short-range force (Born repulsion force), making sure that particles cannot collide. We use a formula derived by Feke et al. [24],

$$V_{\text{Born}} = \frac{AN}{\tilde{R}}\left(\frac{\tilde{R}^2-14\tilde{R}+54}{(\tilde{R}-2)^7} + \frac{60-2\tilde{R}^2}{\tilde{R}^7} + \frac{\tilde{R}^2+14\tilde{R}+54}{(\tilde{R}+2)^7}\right). \quad (7)$$

In this expression $\tilde{R}=R/a$ is the ratio of the center-center distance and the particle radius. As discussed by Feke et al. [24] N lies in the interval 10^{-18} to 10^{-23}. In our simulations we used $N=10^{-23}$. Figure 1 shows the interaction potential
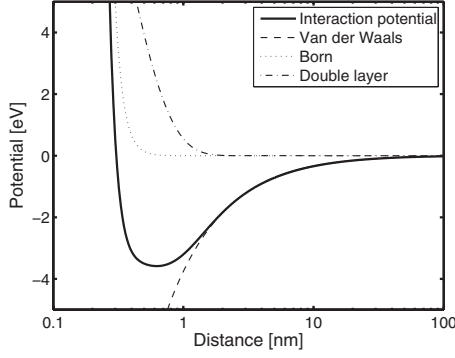
FIG. 1. Interaction potential between two equal spherical particles of radius $a=0.735$ μm. The potential comprises attractive van der Waals interactions with a Hamaker constant of $A=0.062$ eV, repulsive electrostatic interactions in a 150 mM $MgCl_2$ aqueous solution, a surface potential of $\phi_0=40$ mV, and the Born repulsion where N is assumed to be $N=10^{-23}$.

between two particles for conditions corresponding to the experiments by Pantina and Furst [21]. As expected for this parameter set, the aggregation of particles is not hindered by an energy barrier and the colloid is in the regime of fast coagulation [4]. The equilibrium surface-surface distance, that is the position of the potential minimum, is typically in the order of some Ångstrom.

IV. TANGENTIAL-FORCE MODEL

A. Model

There is quite a number of tangential-force models available for DEM simulations. For example, the models by Haff and Werner [25], Walton and Brown [26] or Cundall and Strack [5]. For some detail on these models the reader is referred to [27]. For this work the main deficiency of all these models is that most of them are not capable of supporting bending moments between bonded particles, except the ones which will be discussed and compared to our model in Sec. IV C. In the following we propose a tangential-force model, similar to that by Cundall and Strack, which can reproduce the phenomena described in Sec. II. In the Cundall-Strack model a spring $\boldsymbol{\xi}_{ij}$ with rigidity k_t will be initialized when two particles, i and j, get into contact. This spring grows proportional to the relative tangential velocity at the contact point,

$$\boldsymbol{\xi}(t) = \int_{t_0}^{t} dt' \boldsymbol{v}_t(t') \Rightarrow \dot{\boldsymbol{\xi}} = \boldsymbol{v}_t. \tag{8}$$

Here t_0 is the time when the particles get into contact. The relative tangential velocity is given by

$$\boldsymbol{v}_t = (\boldsymbol{v}_j - \boldsymbol{v}_i)_t + a(\boldsymbol{\omega}_j + \boldsymbol{\omega}_i) \times \boldsymbol{n}_{ij}, \tag{9}$$

where $\boldsymbol{n}_{ij}$ is defined as $(\boldsymbol{r}_j - \boldsymbol{r}_i)/|\boldsymbol{r}_j - \boldsymbol{r}_i|$. The subscript t denotes the projection of the relative velocity onto the tangential plane. If the force due to the tangential spring exceeds an upper bound, which in the work by Cundall and Strack [5] is the Coulomb friction μF_n, the spring will be set to
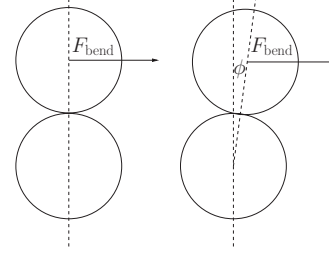

FIG. 2. Example for the bending torque, the lower particle is fixed and on the upper particle acts as a tangential force (left-hand side). If the bond between the particles is able to support a bending moment, a stationary angle $\phi < \pi/2$ between the original contact line and the stationary contact line should be reached.

$$\boldsymbol{\xi} = \mu \frac{F_n}{k_t} \frac{\boldsymbol{\xi}}{|\boldsymbol{\xi}|}, \tag{10}$$

where μ is the friction coefficient. To make sure that the tangential force acts only in tangential direction, the Cundall-Strack spring is mapped to the tangential plane perpendicular to $\boldsymbol{n}_{ij}$ after each time step. The tangential forces and torques acting on the ith and the jth particle are given by

$$\boldsymbol{F}_{t,i} = k_t\boldsymbol{\xi}, \quad \boldsymbol{M}_i = R_i\boldsymbol{F}_{t,i} \times \boldsymbol{n}_{ij}, \tag{11}$$

$$\boldsymbol{F}_{t,j} = -k_t\boldsymbol{\xi}, \quad \boldsymbol{M}_j = -R_j\boldsymbol{F}_{t,j} \times \boldsymbol{n}_{ij}. \tag{12}$$

This model is able to capture a lot of phenomena such as sliding friction and sticking friction. However, it is not able to support a bending moment between two bonded particles, which becomes obvious by the following example. We assume a fixed (no translation or rotation) particle bonded to a second particle as sketched in Fig. 2. An external force perpendicular to the center-center line of the particles acts on the second particle. Now we look for a static solution of the evolution equations, in which all resulting forces and moments have vanished. From Eqs. (11) and (12) immediately follows that this is only the case if $\boldsymbol{\xi}=0$. This in turn means that the whole external force must be equilibrated by the normal forces between the particles and this can only be the case if the center-center line is finally parallel to the direction of the external force. However, this means that the bond cannot support any bending moment. In order to derive a similarly simple model, however capable of supporting bending moments, we use the following reasoning: When two particles get in contact, we introduce two thought rods rigidly connected to one particles center and reaching to the center of the other particle as sketched in Fig. 3. Between the end point of the rod and the center of the other particle a spring will be initialized. This spring grows proportional to the relative tangential velocity between the rods end points and the particle center. The evolution equations for the springs are then

$$\dot{\boldsymbol{\xi}}_{ij} = (\boldsymbol{v}_j - \boldsymbol{v}_i)_t - (\boldsymbol{\omega}_i \times \boldsymbol{n}_{ij})2a, \tag{13}$$
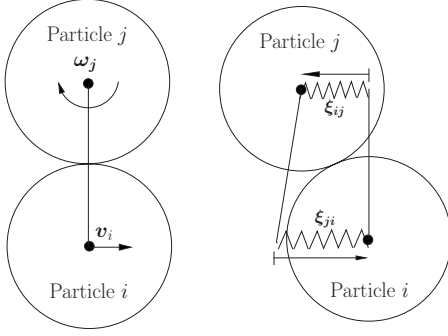
FIG. 3. Sketch of tangential-force model. (a) When two particles get in contact, two thought rods are initialized. The rods are rigidly connected to the center of one particle and reach the other particles center. (b) According to the tangential movement of the particles, the springs $\boldsymbol{\xi}_{ij}$ and $\boldsymbol{\xi}_{ji}$ will be elongated. The arrows denote the direction of the vectors $\boldsymbol{\xi}_{ij}$ and $\boldsymbol{\xi}_{ji}$.

$$\dot{\boldsymbol{\xi}}_{ji} = (\boldsymbol{v}_i - \boldsymbol{v}_j)_t + (\boldsymbol{\omega}_{\mathbf{j}} \times \boldsymbol{n}_{ij})2a, \tag{14}$$

where $\boldsymbol{\xi}_{ij}$, $\boldsymbol{\xi}_{ji}$ are defined in Fig. 3. The forces and moments acting on the particles are therefore

$$\boldsymbol{F}_i = k_t(\boldsymbol{\xi}_{ij} - \boldsymbol{\xi}_{ji}), \quad \boldsymbol{M}_i = 2ak_t\boldsymbol{n}_{ij} \times \boldsymbol{\xi}_{ij}, \tag{15}$$

$$\boldsymbol{F}_j = k_t(\boldsymbol{\xi}_{ji} - \boldsymbol{\xi}_{ij}), \quad \boldsymbol{M}_j = -2ak_t\boldsymbol{n}_{ij} \times \boldsymbol{\xi}_{ji}. \tag{16}$$

Equivalent to the Cundall-Strack model both tangential springs are mapped to the plane perpendicular to $\boldsymbol{n}_{ij}$ after each time step. The springs stop extending if its elongation exceeds a maximum value ξ_{max}. Unlike the model of Cundall and Strack, this model is able to support bending moments. Let us demonstrate that by the same example as above.

By solving the steady-state equations one finds in the case of small deflections for the reorientation angle ϕ,

$$\phi = \frac{F_{Bend}}{k_t 2a}. \tag{17}$$

Note that our model has some similarity to a theoretical approach introduced in [28] where a random network of springs (normal and tangential) was used to predict the elastic moduli for disordered packings of interconnected spheres. Here the tangential spring stiffness was determined by the predictive model of Pantina and Furst [21,22].

We assume the model to be valid also for nontenuous aggregates as long as pairwise contact forces can be assumed. In this contribution we content ourselves with polymeric primary particles as investigated in [21]. Whether our model is also applicable to other types of particles (e.g., inorganic and surfactant-coated colloids) cannot be revealed by the model itself but must be clarified experimentally.

B. Parameter determination

The introduced model contains two parameters. The spring stiffness k_t and the maximum spring length ξ_{max}. Both parameters can be determined by the experiments presented in [21]. As shown in Appendix B the static shape of a linear chain of particles under a bending stress is given in leading order approximation by

$$\frac{y(x)}{F_{Bend}} = -\frac{1}{8a^3k_t}\left(\frac{L}{4}x^2 - \frac{|x|^3}{6}\right), \tag{18}$$

where L is the center-center distance of the first and the last particle in the chain. By comparison with Eq. (1) one finds

$$EI = 8a^3k_t. \tag{19}$$

From the elongation of the chain, $\delta = y(0) - y(L/2)$, one finds by comparison with Eq. (2) $\kappa = 192(a/L)^3 k_t$ and therefore from (3),

$$k_t = \frac{\kappa_0}{192}. \tag{20}$$

Using Eq. (20) one directly obtains the model parameter for the tangential stiffness k_t from the measured value κ_0. The value of ξ_{max} can be obtained from the measurement of the critical bending moment M_c in [21]. The bending torque acting on a particle is given by Eq. (15) or (16). Since $\boldsymbol{n}_{ij}$ and $\boldsymbol{\xi}_{ij}$ are perpendicular to each other ξ_{max} must be

$$\xi_{max} = \frac{M_c}{2ak_t}. \tag{21}$$

Thus, all parameters of the force model can be determined from experimental data. Alternatively, the predictive formulas derived by Pantina and Furst [21,22] for the single bend rigidity κ_0 may be used to estimate the model parameters.

C. Comparison to other models

In [18] a model derived by Kantor and Webman [14] was applied to computer simulations of two-dimensional colloidal aggregates in shear flows. That model assumes that the contribution of tangential deformation to the strain energy is proportional to

$$E \propto \sum_{i,j,k} \delta\Phi_{ijk}^2, \tag{22}$$

where $\delta\Phi_{ijk}$ is the change in the angle between the bonds (i,j) and (i,k) connected to particle i. The contribution to the interaction force can be described by

$$\boldsymbol{F}_{ij} = -\beta\sum_k \delta\Phi_{ijk}\boldsymbol{n}_{ik} \cdot (\boldsymbol{n}_{ij} \cdot \boldsymbol{n}_{ik}). \tag{23}$$

It is mentioned in [18] that a chain of particles connected by such forces behaves like a thin elastic rod with the same length. As shown in Appendix A, our model leads in the case of a linear structure (i.e., every particle is bonded to a maximum of two other particles) to an elastic equilibrium energy of

$$E = a^2k_t\sum_i \delta\Phi_i, \tag{24}$$

where $\delta\Phi_i$ denotes the change of the angle between the two bonds ending on particle i. Due to the fact that (24) and (22) are equivalent, the equilibrium elastic deformation of our model is also equivalent.

The main difference between the two models is that our model takes only pairwise interactions into account, while

the model by Kantor and Webman [14] is a three particle interaction model. The tangential forces and the bending energy are there related to the change of angles between neighboring bonds. However, one would expect that the energy is stored directly in the bonds. It remains unclear why the angle between two different bonds is the measure for the elastic energy. Although the same behavior is observed in our proposed model, the reason is quite obvious. The energy is directly stored in the bonds but neighboring bonds are related due to the equilibrium conditions. In contrast to the model of Kantor and Webman the proposed model is suited to describe nonelastic displacements of the bonds, which occur if the maximum supported bending moment is reached. Furthermore, the tracking of angles between all bonds ending on the same particle may cause much higher implementatory (and possibly computational) effort compared to the proposed model.

To avoid the computational problems caused by tracking of the angles, West, Melrose, and Ball [19] proposed a model where the basic colloidal unit is replaced by a trimer of stiff spheres and the interactions are assumed as superposition of 3×3 pairwise interacting central forces. Depending on the relative orientation of the trimers, bonds between two trimers are able to support bonding moments. Contrary to our proposed model this only provides qualitative information. Besides, no relation between experimental data and model parameters is available. Furthermore, replacing one particle by three particles leads to a higher computational effort. Nevertheless, the ansatz of West, Melrose, and Ball is probably superior to our model for the simulation of colloids containing nonspherical primary particles.

The model of Botet and Cabane [20] is in principle able to capture the effect observed by Pantina and Furst [21]. They modeled the interactions between two spheres by a number of springs connected to pins which are randomly distributed over the spheres. In comparison to our model the model of Botet and Cabane [20] consumes much more computational resources in order to handle the pins and springs. Furthermore, the estimation of the model parameters, i.e., number of pins, spring stiffness, equilibrium, and breakage lengths, seemed to be more difficult.

V. SIMULATION METHOD AND RESULTS

We assume spherical monodisperse colloidal particles immersed in an aqueous $MgCl_2$ solution. Unless otherwise noted we used the parameters from [21]. The radius of the particles is $a = 0.735$ μm. The surface potential is $\phi_0 = 40$ mV. We use the discrete element method [5,6] to simulate aggregate structure evolution. The main idea of this method is to track the trajectories of all primary particles by solving Newton's equations of motion numerically. In general the state of the particle system is given by the particle positions $\{r_1, r_2, \ldots, r_N\}$, velocities $\{v_1, v_2, \ldots, v_n\}$, and by the angular velocities $\{\omega_1, \omega_2, \ldots, \omega_n\}$. Note that there is no need to track the particles' orientation angles as we content ourselves with spherical particles. For the interactions between the fluid and the particles we use the free draining approximation: Every particle experiences the unperturbed

flow field as if no other particle were in the flow. The drag force and torque acting on the ith particle is then given by Stokes formulas [29]

$$F_{\text{drag},i} = 6\pi\eta a[v_i - u(r_i)], \tag{25}$$

$$M_{\text{drag},i} = 8\pi\eta a^3[\omega_i - \Omega(r_i)]. \tag{26}$$

With η, v_i, and $u(r_i)$ being the dynamic viscosity of the carrier fluid, the velocity of ith particle, and the fluid velocity at the position of ith particle, respectively. $\Omega = 1/2\nabla \times u$ is the vorticity of the fluid velocity field. For the considered particles, effects of inertia can surely be neglected. Therefore, the particle dynamic is governed by the overdamped equations of motion,

$$\dot{r}_i = \frac{1}{6\pi\eta a}F_i + u(r_i), \tag{27}$$

$$\omega_i = \frac{1}{8\eta\pi a^3}M_i + \Omega(r_i). \tag{28}$$

The forces F_i and the torques M_i include all interaction effects acting on the ith particle. For solving the equations of motion we use Heun's method, which has a global error of order Δt^2 and is similar to the velocity-Verlet method, often used in molecular dynamics and DEM simulations [30]. Note that the velocity-Verlet method itself is explicitly designed for solving Newton's equations of motion and cannot be used in overdamped dynamics. In principle, we can use the force models described above to simulate the colloid. However, from the slope of the potential plot (Fig. 1) a computational problem becomes apparent. In the neighborhood of the potential minimum the interaction forces change rapidly on very small length scales. Therefore, it is necessary to solve the equations of motion with very small time steps to track the details of motion and avoid instabilities of the numerical solution. We found that the magnitude of time steps must approximately be 10^{-9} s to track particle motion correctly. However, if two particles are bonded to each other, the center-center distance remains approximately constant and only the angular orientation of the particles can change significantly. In order to avoid the need of such small time steps we introduce a constraint if the distance between two particles i and j becomes smaller than a critical distance d_c. The equations of motion are then solved with the constraint $|r_i - r_j| = d_c$. For solving the constrained equations of motion, we adopted the RATTLE algorithm derived by Andersen [31], which fulfills the constraint up to a given tolerance (tol), to Heun's method. In this paper we used $d_c = 1.1$ nm and tol equal to 0.1 nm. By careful investigation of numerical results we found that the value of d_c has a negligible effect on the results to be presented below as long as d_c is much smaller than the primary particles' radius a. With the chosen parameters we were able to use time steps of the order of 10^{-6} s, which leads to remarkable improvements in simulation time. However, the time needed by the Anderson algorithm is proportional to the number of bonds in the aggregate, and especially for large compact structures, the com-
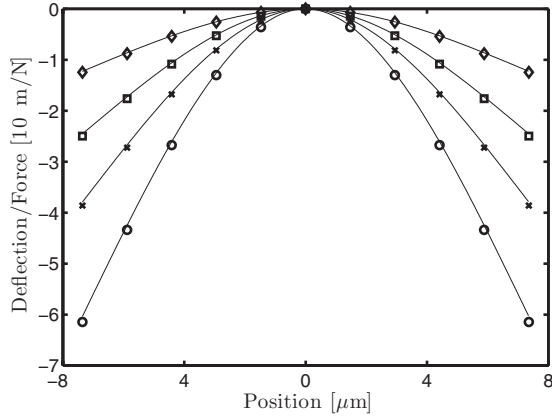
FIG. 4. Simulated shape of a bended 11-particle aggregate for different material parameters. The used tangential stiffness are k_t =0.785 mN/m (circles), k_t=1.1 mN/m (crosses), k_t=1.7 mN/m (squares), and k_t=3.4 mN/m (diamonds). The symbols are simulation results and the lines are obtained from (1).
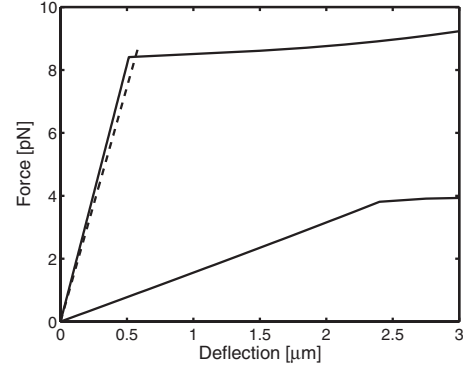

FIG. 5. Typical deflection-force curves for a 11-particle (upper line) and a 23-particle aggregate (lower curve). The parameters for the tangential-force model are k=0.69 mN/m and ξ_{max}=30.48 nm obtained from measured data in [21] for a 150 MgCl₂ solution. The dashed line shows the experimentally obtained linear part of the deflection-force curve taken from a data plot (Fig. 2) presented by [21].

putation time may grow fast with the number of particles used in the simulation.

In order to reproduce the results of Pantina and Furst, we performed simulations where a linear chain of particles is bended. We applied an external force F_{Bend} directed perpendicular to the chain of particles to the middle particle. We compensate this force by applying $-F_{Bend}/2$ on the terminal particles of the chain. Then we run the simulation until the static shape is achieved. Note that the value of the fluid viscosity has no influence on the static solution, but only on the time needed to achieve it. Figure 4 shows simulated deflection curves for an aggregate comprising of 11 particles for different spring stiffness k_t=0.69, 1.1, 1.7, 3.4 mN/m. These values correspond to the measured κ_0 for different MgCl₂ concentrations (150, 250, 375, 500 mM, respectively) [21]. All four curves are well described by Eq. (1) (solid lines) with EI obtained from Eq. (20).

Figure 5 shows typical deflection vs force curves. Here the measured value of κ_0=0.13 N/m for a 150 mM MgCl₂ concentration was used [21]. For small deflections, the aggregate is bended similar to a rigid rod as described above. In that regime the deflection vs force curve shows a linear behavior. If the bending force exceeds a critical value, rearrangement of the particles occurs. Beyond this point, the particles form a near triangular structure. The simulation results in the linear regime and the critical force where the rearrangement occurs are in agreement with the experimental data presented in [21] (Fig. 2). Note that for experimental reasons the relevant part of the data presented by [21] are on a deflection interval of approximately. 1.5–2 μm. The reason is some tortouisity in the chains, which must be unbend before the linear elongation regime starts [35]. The simulated behavior after reaching rearrangement is different from the experimental data. This is due to the fact that the terminal particles in the experiment are trapped by optical tweezers while in the simulation only a force perpendicular to the linear chain direction is applied. The behavior of both setups is comparable as long as the particles' displacements in x direction are small. However, this is no longer the case if the

rearrangement to triangular structures has occurred.

Finally, we used our simulation to track the time evolution of an aggregate comprising 200 primary particles in a resting fluid. The initial aggregate was obtained by diffusion-limited cluster particle aggregation [32]. We compared the results by using the classical DLVO forces only with the results obtained using our tangential-force model. Figure 6 shows the initial aggregate and the restructured aggregate after 25 s using DLVO forces only. It is remarkable that even in a resting fluid the aggregate collapses to a more compact structure. This behavior obviously is a result of the used force models. The van der Waals forces act over a relatively long range. As there is no resistance of single particle bonds against bending moments, the bonded particles can freely reorient. This behavior contradicts the observation that fractal structure are
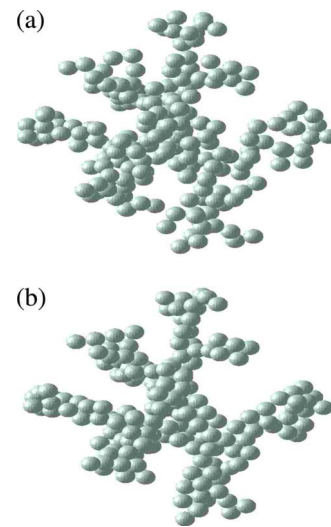

FIG. 6. (Color online) Compaction of an aggregate using central forces only. (a) The start configuration, generated by diffusion-limited aggregation. (b) The configuration after a simulated time period of 25 s, the structure is significantly more compact than the starting configuration.
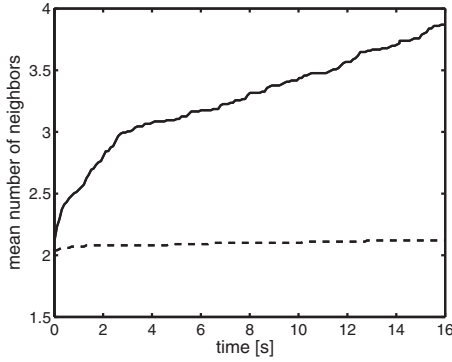
FIG. 7. Time evolution of the average number of neighbors. The solid line shows simulation results where DLVO forces only were considered. The dashed line displays data obtained from simulations where the tangential-force model was applied.

often stable over long times even in moderate shear flows [33,34]. This indicates that assuming purely central forces is an over-simplification which hinders the prediction of realistic structure evolution. Under the same conditions, but using the introduced tangential-force model, the compaction does not occur. In order to quantify the compaction of the aggregate we count the number of neighboring particles for each particle. The average number of neighbors is used as a measure for the compactness. Particles are considered to be neighbors if their surface-surface distance is below 10 nm. Note that we deliberately do not use the fractal dimension as a measure for compactness because the aggregate loses the property of self-similarity during the compaction process. Figure 7 shows the time evolution of the average number of neighbors for the case of using DLVO forces only and for the case of using DLVO augmented with our tangential model. In case of using DLVO only, the number of neighbors grows continuously, while the compaction of the aggregate is negligible if the tangential model is used.

VI. SUMMARY AND CONCLUSION

In this work we have introduced a model for tangential interaction forces applicable in computer simulations. Our tangential-force model is capable of supporting bending moments. This is an important quality as it has been recently shown experimentally that colloidal bonds actually support bending moments [21]. Our model is based on two tangential springs acting between bonded particles. The time evolution of these springs is determined by the relative tangential velocity between the particles. The spring elongation is constrained to a maximum elongation to account for sliding effects. The model contains two parameters: The stiffness of the springs and the maximum elongation. We showed that both parameters can be determined directly from the experiments shown in [21] and simulations using our model are able to reproduce the experimental observations. We compared our model to former models which were used in computer simulations and are capable of supporting bending moments. Furthermore, we showed that even in the case of simulating a fractal aggregate in a resting fluid, models with-
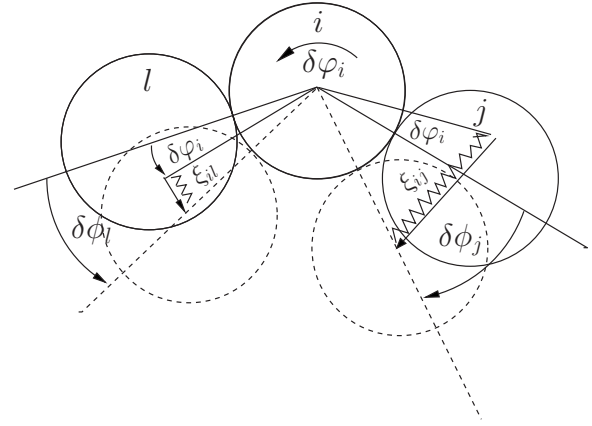

FIG. 8. Sketch for the calculation of the bending energy. The initial configuration is shown by solid lines. After the deformation process the three particles have new positions and orientations, shown by the dashed lines. The particles l and j are reoriented relative to particle i by the angles $\delta\phi_l$ and $\delta\phi_j$, and particle i was rotated around its center by the angle $\delta\varphi_i$. The springs ξ_{ij} and ξ_{il} are deformed due to the particle motion.

out tangential forces lead to an unrealistic collapse of the aggregate. Using our tangential-force model can remedy that flaw.

APPENDIX A: DETERMINATION OF THE EQUILIBRIUM BENDING ENERGY IN LINEAR STRUCTURES

In order to determine the bending energy in a linear structure of particles we consider three particles l, i, and j of a structure which undergoes deformations as sketched in Fig. 8. The torque balance for particle i follows from Eq. (15),

$$0 = 2ak_t(\boldsymbol{\xi}_{il} \times \boldsymbol{n}_{il} + \boldsymbol{\xi}_{ij} \times \boldsymbol{n}_{ij}). \tag{A1}$$

Assuming small deformations, Eq. (A1) can be rewritten as a scalar equation,

$$\xi_{il} - \xi_{ij} = 0. \tag{A2}$$

Under the assumption that all deflections are small and no plastic deformation occurs during deformation (i.e., no spring length in the system exceeded ξ_{max}) one finds from Eq. (13),

$$\xi_{il} = 2a(\delta\phi_l - \delta\varphi_i), \tag{A3}$$

$$\xi_{ij} = 2a(\delta\phi_j + \delta\varphi_i). \tag{A4}$$

Introducing this in Eq. (A2) and solving the resulting equation for $\delta\varphi_i$ leads to

$$\delta\varphi_i = \tfrac{1}{2}(\delta\phi_l - \delta\phi_j). \tag{A5}$$

The energy stored in the springs ξ_{il} and ξ_{ij} is given by
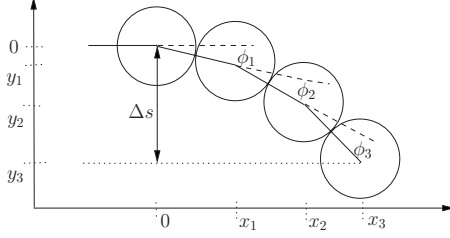
FIG. 9. Sketch for the calculation of the equilibrium shape.

$$E_i = \frac{1}{2} k_t (\xi_{il}^2 + \xi_{ij}^2). \tag{A6}$$

Introducing (A3) and (A4) in (A6) leads to the equation

$$E_i = 2a^2 k_t (\delta\phi_l^2 + \delta\phi_j^2 + 2\delta\varphi_i(\delta\phi_j - \delta\phi_l) + 2\delta\varphi_i^2). \tag{A7}$$

By introducing Eq. (A5) in (A7) one obtains

$$E_i = a^2 k_t (\delta\phi_l + \delta\phi_j)^2. \tag{A8}$$

This in turn can be expressed as the change of the angle between the bond of particles l and i and particles i and j, $\delta\Phi = \delta\phi_1 + \delta\phi_2$. Therefore, we obtain

$$E_i = a^2 k_t \delta\Phi^2. \tag{A9}$$

By adding E_i for all particles in the chain one gets the whole elastic energy of the structure, except the contribution from rods rigidly connected to terminal particles to a particle within the structure. Therefore, E_i can be understood as the energy per particle in an elastic deformed linear structure of colloidal particles.

APPENDIX B: DETERMINATION OF THE EQUILIBRIUM SHAPE

In order to calculate the shape of a bended chain of particles as described in Sec. IV B, we minimize the elastic energy stored in such an elastic chain. From symmetry reasons it is sufficient to consider only one-half of the chain. As shown in Fig. 9 the change in the angle of the bonds connected to the nth particle is denoted as ϕ_n. The bending energy per particle is therefore given by (A9),

$$E_n = a^2 k_t \phi_n^2. \tag{B1}$$

The elastic energy stored in the whole chain is therefore

$$E = 2 \sum_{i=1}^{N-1} a^2 k_t \phi_n^2, \tag{B2}$$

where N is the number of particles in one-half of the chain.

In equilibrium this energy should be minimal. The position of the nth particle is

$$y_n = -2a \sum_{i=1}^{n} \sin\left(\sum_{j=1}^{i} \phi_j \right). \tag{B3}$$

Assuming small total deflection this reduces to

$$y_n = -2a \sum_{i=1}^{n} \sum_{j=1}^{i} \phi_j. \tag{B4}$$

Assuming that the total deflection of the rod is Δs we have a constraint for the energy minimization,

$$\Delta s = 2a \sum_{i=1}^{N-1} \sum_{j=1}^{i} \phi_j. \tag{B5}$$

Using the technique of Lagrangian multiplier we must minimize the quantity,

$$E = \sum_{i=1}^{N-1} 2a^2 k_t \phi_n^2 - \lambda \left(2a \sum_{i=1}^{N-1} \sum_{j=1}^{i} \phi_j + \Delta s \right), \tag{B6}$$

where λ is the Lagrangian multiplier. To minimize E one must solve

$$0 = \frac{dE}{d\phi_m} = 4a^2 k_t \phi_m - 2\lambda a \sum_{i=1}^{N-1} \sum_{j=1}^{i} \delta_{j,m}, \tag{B7}$$

where $\delta_{j,m}$ is the Kronecker symbol which is equal to one if $j=m$ and zero elsewhere. The solution of this equation is

$$\phi_m = \frac{\lambda(N-m)}{2ak_t}. \tag{B8}$$

Introducing this in the constraint (B5) one finds after some algebra

$$\frac{\lambda}{k_t} \left(\frac{1}{3} N^3 - \frac{1}{2} N^2 + \frac{1}{6} N \right) = \Delta s. \tag{B9}$$

Under neglecting all powers of N smaller than 3 one finds

$$\lambda = \frac{3k_t \Delta s}{N^3}, \tag{B10}$$

and by introducing that in Eq. (B8),

$$\phi_m = \frac{3}{2} \frac{\Delta s}{aN^3}(N-m). \tag{B11}$$

Introducing this in Eq. (B4), using $N=L/4a$, $m=x_m/a$, and neglecting all terms that vanish for $a \to 0$ one finds

$$y_m = \frac{\Delta s}{L^3}(6x_m^2 - 4|x_m|^3). \tag{B12}$$

Introducing (B8) in (B2) results in an expression for the elastic energy as a function of N or L, respectively, and Δs. The bending force is related to that energy by

$$F_{\text{Bend}} = \frac{dE}{d\Delta s}. \tag{B13}$$

Now one can eliminate Δs. After introducing Δs in (B12) the elongation is found,

$$y_m = \frac{F_{\text{Bend}}}{8a^3 k} \left(\frac{L}{4} x_m^2 - \frac{1}{6} |x_m|^3 \right). \tag{B14}$$

[1] M. Doi and D. Chen, J. Chem. Phys. **90**, 5271 (1989).

[2] D. Chen and M. Doi, J. Chem. Phys. **91**, 2656 (1989).

[3] K. Higashitani, K. Iimura, and H. Sanda, Chem. Eng. Sci. **56**, 2927 (2001).

[4] J. R. Hunter, *Foundations of Colloid Science*, 5th ed. (Oxford Science, Oxfrod 1995).

[5] P. A. Cundall and O. D. L. Strack, Geotechnique **29**, 47 (1979).

[6] P. Poeschel and T. Schwager, *Computational Granular Dynamics: Models and Algorithms*, 2nd ed. (Springer, Berlin, 2005).

[7] M. Fanelli, D. L. Feke, and I. Manas-Zloczower, Chem. Eng. Sci. **61**, 4944 (2006).

[8] M. Fanelli, D. L. Feke, and I. Manas-Zloczower, Chem. Eng. Sci. **61**, 473 (2006).

[9] S. Harada, R. Tanaka, H. Nogmi, M. Sawada, and K. Asakura, Colloids Surf., A **302**, 396 (2007).

[10] L. Durlofsky, J. F. Brady, and G. Bossis, J. Fluid Mech. **180**, 21 (1987).

[11] J. F. Brady and G. Bossis, Annu. Rev. Fluid Mech. **20**, 111 (1988).

[12] S. Feng, P. N. Sen, B. I. Halperin, and C. J. Lobb, Phys. Rev. B **30**, 5386 (1984).

[13] S. Feng and P. N. Sen, Phys. Rev. Lett. **52**, 216 (1984).

[14] Y. Kantor and I. Webman, Phys. Rev. Lett. **52**, 1891 (1984).

[15] L. M. Schwartz, S. Feng, M. F. Thorpe, and P. N. Sen, Phys. Rev. B **32**, 4607 (1985).

[16] A. A. Potanin, J. Chem. Phys. **96**, 9191 (1992).

[17] M. Born and K. Huang, *Dynamical Theory of Crystal Lattices* (Oxford University, New York, 1954).

[18] A. A. Potanin, J. Colloid Interface Sci. **157**, 399 (1993).

[19] A. H. L. West, J. R. Melrose, and R. C. Ball, Phys. Rev. E **49**, 4237 (1994).

[20] R. Botet and B. Cabane, Phys. Rev. E **70**, 031403 (2004).

[21] J. P. Pantina and E. M. Furst, Phys. Rev. Lett. **94**, 138301 (2005).

[22] J. P. Pantina and E. M. Furst, Langmuir **22**, 5282 (2006).

[23] J. Israelachvili, *Intermolecular and Surface Forces*, 2nd ed. (Academic, New York, 1994).

[24] D. L. Feke, N. D. Prabhu, and J. A. Mann, J. Chem. Phys. **88**, 5735 (1984).

[25] P. K. Haff and B. T. Werner, Powder Technol. **48**, 239 (1986).

[26] O. R. Walton and R. L. Braun, J. Rheol. **30**, 949 (1986).

[27] H. Kruggel-Emden, S. Wirtz, and V. Scherer, Chem. Eng. Sci. **63**, 1523 (2008).

[28] A. Zaccone, M. Lattuada, H. Wu, and M. Morbidelli, J. Chem. Phys. **127**, 174512 (2007).

[29] L. D. Landau and E. M. Lifschitz, *Lehrbuch der theoretischen Physic, Band VI Hydrodymik*, 5th ed. (Akademie, Verlag, Gmbh, 1993).

[30] D. Frenkel and B. J. Smit, *Understanding Molecular Simulation* (Academic, New York, 2002).

[31] H. C. Andersen, J. Comput. Phys. **52**, 24 (1983).

[32] T. A. Witten and L. M. Sander, Phys. Rev. B **27**, 5686 (1983).

[33] C. Selomulya, R. Amal, G. Bushell, and T. D. Waite, J. Colloid Interface Sci. **236**, 67 (2001).

[34] C. Selomulya, G. Bushell, R. Amal, and T. D. Waite, Langmuir **18**, 1974 (2002).

[35] E. M. Furst (private communication).